

# Coexistence of bunching and meandering instability in simulated growth of 4H-SiC(0001) surface

Filip Krzyżewski\*

*Institute of Physics, Polish Academy of Sciences, Al. Lotników 32/46, 02-668 Warsaw, Poland*

Magdalena A. Załuska-Kotur†

*Institute of Physics, Polish Academy of Sciences, Al. Lotników 32/46,  
02-668 Warsaw, Poland and Faculty of Mathematics and Natural Sciences,  
Card. Stefan Wyszyński University, ul Dewajtis 5, 01-815 Warsaw, Poland*

(Dated: March 31, 2014)

Bunching and meandering instability of steps at the 4H-SiC(0001) surface is studied by the kinetic Monte Carlo simulation method. Change in the character of step instability is analyzed for different rates of particle jumps towards step. In the experiment effective value of jump rates can be controlled by impurities or other growth conditions. An anisotropy of jump barriers at the step influences the character of surface structure formed in the process of crystal growth. Depending on the growth parameters different surface patterns are found. We show phase diagrams of surface patterns as a function of temperature and crystal growth rate for two different choices of step kinetics anisotropy. Jump rates which effectively model high inverse Schwoebel barrier (ISB) at steps lead either to regular, four-multistep or bunched structure. For weak anisotropy at higher temperatures or for lower crystal growth rates meanders and mounds are formed, but on coming towards lower temperatures and higher rates we observe bunch and meander coexistence. These results show that interplay between simple dynamical mechanisms induced by the asymmetry of the step kinetics and step movement assisted by the step edge diffusion are responsible for different types of surface morphology.

PACS numbers: 05.10, 61.82Fk, 81.10Aj

## I. INTRODUCTION

Silicon carbide (SiC) is intensively studied material due to its application in high temperature, high power and high frequency electronic devices. Lately it became even more interesting as a basis for graphene production. Being the matter of continuous interest it is the subject of many experimental as well theoretical investigations. Depending on growth conditions many various step patterns as multisteps, bunches or meanders at SiC surface were seen. The morphological instability of step trains during growth of 6H-SiC(0001) [1–8] and 4H-SiC(0001) [9–14] surfaces were studied in various experimental conditions. It was observed that such instability can be impurity induced and the mechanism of this influence can be related to the change of the effective jump barriers at the steps [1, 2].

Complex morphological features at the growing crystal surface follow from an interplay among nucleation, diffusion, and the incorporation of adatoms at steps [15–17]. It was shown that the balance between the flux of adparticles attaching step from the upper terrace and flux from the lower terrace has key impact on the step stability and the emergence of the final surface pattern [17–19]. During crystal growth or sublimation process various factors

may affect the fluxes. The most often discussed reason for imbalanced fluxes is so called Schwoebel barrier (SB) at steps [18]. Similar effect onto the step stability has the step movement during crystal growth or sublimation process [20, 21]. The inverse Schwoebel barrier (ISB) acts in the opposite direction that usual SB slowing flux that comes towards the step from the lower terrace and it can stop or invert the effects of the natural asymmetry in step dynamics. These two factors: ISB and step movement during crystal growth induce particle fluxes in the opposite directions. Step movement appears to be quite effective mechanism to generate step bunching in the process of crystal annealing [20–22] and the presence of ISB is an origin of bunches during crystal growth [15]. SB is known as a reason for step meandering instability at surfaces of grown crystals [17, 19], however the step meandering due to the diffusion along step edges either via kink Schwoebel barrier [23–25] or via unhindered step-edge diffusion [26] often overcomes SB effect.

All particle fluxes either along surface or along step edges depend on the growth parameters like temperature and growth rate. They follow in different way changes of parameters and as an effect various surface patterns are created. The analysis of experimentally observed bunching process at SiC(0001) surface indicates that the impurity adsorption influences the final step pattern of growing crystal [1, 2]. It was argued that the nitrogen adsorbed at steps can enhance the incorporation rate of adatoms from the upper terraces or reduce that from the lower terraces [1, 2], thus changing the value of effective

---

\*Electronic address: fkrzy@ifpan.edu.pl

†Electronic address: zalum@ifpan.edu.pl

ISB. We show concrete examples of step patterns that result as a competition of ISB and step rate at different growth conditions. Temperature - rate pattern diagram changes for different choices of ISB height.

Evolution of 4H-Si(0001) surface is modeled by use of kinetic Monte Carlo simulations [27–30] and bunching - meandering instability is studied as a function of temperature and the crystal growth rate for different ISB values. We show that with high ISB value steps create bunches at low temperatures which depending on the step rate changes into 4-step patterns or regular step arrangement. When ISB is absent no step bunching happens and only meandered, 4-step and mound structures are build. The situation is different for low ISB values. Depending on the temperature we observe 4-step structures or regular in-phase meanders, which change into mounds or bunch and meanders coexistence for higher step rates. This last structure is very similar to the one seen experimentally in Ref. 31 and obtained in Ref. 32, 33 by phase-field approach. It is simultaneous bunch and meandered structure, an intermediate ordering between bunches and meanders. In our case we realize such structure by the presence of ISB, which is not so large to win over the flux up the steps in the whole area, but large enough to cause step bunching in some parts of the system.

Our kMC model is described in Sec I, then we discuss results of simulations in Sec II for high ISB and low ISB successively and summarize by conclusions in Sec III.

## II. THE MODEL

Kinetic Monte Carlo (kMC) simulations were carried out on the lattice of 4H politype of silicon carbide. Elementary cell of such a crystal consists of eight alternating layers of Si and C atoms. Consecutive double SiC layers of the lattice are shifted towards each other in order to form ABAC stack which corresponds to the silicon face of polar 4H-SiC crystal structure [27–30]. The surface of 4H SiC(0001) symmetry was modeled. Both silicon and carbon atoms are controlled in the simulation. The energy of grown crystal includes interactions between both types of adatoms

$$H = -E_{\text{SiC}} \sum_{\text{NN}} n_i n_j - E_{\text{SiSi}} \sum_{\text{NNN}} n_i n_j - E_{\text{CC}} \sum_{\text{NNN}} n_i n_j \quad (1)$$

where  $n_i = 0, 1$  means site occupation and sums are over nearest neighboring atom pairs (NN) and next nearest neighbors (NNN). NN bonds are between silicon and carbon atoms and NNN bonds correspond to C-C and Si-Si ones. Energy constants in the formula above are some effective values and can be determined by the analysis of system behavior and by comparing with experimental data for concrete system. We used the same constants that were assumed in Ref.27, where some characteristic features of SiC(0001) kinetics were reproduced. Thus we have  $E_{\text{SiC}} = 0.75\text{eV}$  and  $E_{\text{CC}} = 0.65\text{eV}$  and

$E_{\text{SiSi}} = 0.35\text{eV}$  respectively. Every atom has up to four NNs, which lay in neighboring layers and it is bound with up to twelve NNN. Six of them lay in the same layer, next three one layer below and the last three in the layer above. Geometry and directions of bonds are given by positions of atoms at A, B or C layers forming 4H-SiC crystal.

At the beginning of every simulation system consists of  $N_s$  steps of equal width  $W_s$  which sets the initial mis-cut. Steps ended by silicon alternate with the ones with carbon on the top. The surface is misoriented in  $[01\bar{1}0]$  direction. In the system we set periodic boundary conditions at edges perpendicular to steps and helical boundary conditions for edges parallel to the steps. In order to close such a boundary condition in the correct way, step number  $N_s$  must be divisible by 8. That is the number of monoatomic layers at 4H-SiC elementary cell and also the minimum number of steps to be considered during simulations.

The first step of simulation is an adsorption of silicon and carbon atoms. Probability of such a process is equal to the external particle flux  $F$ ,  $p_A = F$ . In the next step jump directions for each particle at the surface are chosen. Then the probability of a particle diffusion  $p_J$  is calculated. It depends on the system temperature  $T$  as well as on initial  $E_i$  and final  $E_f$  energy of jumping atom calculated as follows

$$E_{i,f} = E_{\text{SiC}} \sum_{(\text{NN})_{i,f}} n_{\text{NN}} + E_{\text{XX}} \sum_{(\text{NNN})_{i,f}} n_{\text{NNN}}. \quad (2)$$

In above formula  $(\text{NN})_{i,f}$  and  $(\text{NNN})_{i,f}$  correspond to nearest and next nearest neighbors of the initial or final particle positions respectively and  $\text{XX}=\text{C}$  C when energy of C atom is calculated and  $\text{XX}=\text{Si}$  Si for Si particle. When the initial energy is higher than the final, the atom jumps from deeper potential well to the shallower one. In this case

$$p_J = \nu \exp(-\beta(E_i - E_f + \Delta_X)), \quad (3)$$

where  $\nu$  is attempt frequency, and  $\beta = 1/k_B T$ ,  $k_B$  is the Boltzmann constant and  $\Delta_X$  with corresponds to the diffusion barrier for C or Si atom ( $X=\text{C}$  or Si). In the case when the initial energy of interactions is lower than the final, hence the atom jumps from shallower to deeper potential well  $p_J = \nu \exp(-\beta\Delta_X)$ . According to several studies barrier for diffusion of carbon atoms is higher [34–36]. We assumed the difference in the diffusion barrier as 0.3 eV. Thus we have  $\Delta_C = 0.3\text{eV}$  for carbon and  $\Delta_{\text{Si}} = 0$  for silicon adatom. Such assumption result in the carbon mobility few times slower than this for silicon adatoms. Silicon diffusion over the surface is the fastest process and sets the time scale of the whole studied kinetics. All other processes are set up relatively to this fastest jump and on assuming that  $\nu = 10^{11}\text{ML/s}$  (monolayer per second) and the barrier for Si diffusion is around 0.8eV we can determine extend of the studied below growth rate, given by  $F$ . We studied fluxes

$F$  within the range of 10 ML/s up to  $10^4$  ML/s (around  $50\text{-}5 \cdot 10^4 \mu\text{m/h}$ ). In such a way we quickly enter area of growth rates which are too high for the experiment. However it is worth noting that all numbers used here are only rough approximation of the real values, and they have their meaning only in qualitative description of behavior of grown crystal. Each of approximated value of parameter can be in fact moved toward higher or lower values, according to some additional data, thus changing range of studied rates and temperatures.

In order to model ISB value an additional barrier  $B_I$  is added for jumps towards and out of neighboring sites. In such a case diffusion close to step edges is slowed down and a formula for the jump probability changes into

$$p_{ISB} = \nu \exp(-\beta(E_i - E_f + \Delta_X + B_I))$$

$$p_{ISB} = \nu \exp(-\beta(\Delta_X + B_I)) \quad \text{for} \quad E_i > E_f \quad (4)$$

In such way incorporation rate of adatoms from upper terrace is different than that from the lower one [37]. Setting an additional barrier at the lower terrace is more effective method to control particle to step fluxes than reduction of barrier at the higher terrace, as it was discussed in Ref 38 and what we have also checked in our simulations.

Each particle at the terrace can desorb from the surface. Probability of that process depends on initial energy of desorbing atom and desorption barrier  $\mu_X$  of silicon  $X = Si$  or carbon  $X = C$ :

$$p_D = \nu_{des} \exp(-\beta(E_i + \mu_X)). \quad (5)$$

In the simulations below we assume  $\nu_{des} = \nu$  and very low desorption rate  $\mu_X = 10\text{eV}$ . Particles practically do not leave the surface.

Simulations begin from the configuration of parallel, equally distanced steps of carbon and silicon layers. Below results for the surface with miscut of  $8^\circ$  are presented. For each studied system we run simulation until several hundreds of layer grow on top of the crystal and observe the shape of stationary pattern that results from the surface kinetics. Different types of the surface patterns found on studying the system kinetics are organized in the temperature - growth rate phase diagram.

### III. BUNCHING AND MEANDERING STEP INSTABILITIES.

#### A. Mechanisms of step instabilities

As long as the particle flux from the upper terrace is balanced with the flux from the lower terrace regular pattern of straight steps is a stable configuration[17, 19, 37]. This situation changes however when these two fluxes achieve different values. Step movement forward during crystal growth or backward during crystal annealing can be the first, natural reason for imbalanced fluxes. Step movement during crystal growth induces advection flux

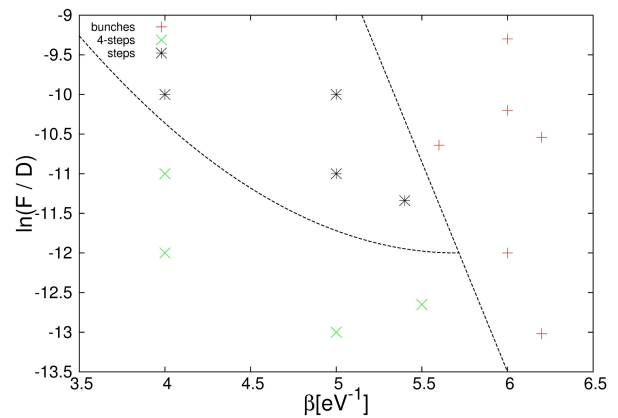


FIG. 1: Diagram of different step patterns at SiC(0001) surface in the  $F/D$  and  $\beta$  plane calculated for the case when  $E_B^{Si} = E_B^C = 0.75\text{eV}$

up the steps and similarly step movement during crystal sublimation gives advection flux down the steps. Crystal growth or sublimation are slow processes and so step rate is slow as compared with the surface diffusion and often it is neglected in the calculations. However as it was shown in Ref. 20, 21 the asymmetry caused by it is comparable to the one in the electromigration process and it is also enough to generate step bunching. On the other hand step movement forward during crystal growth can be natural source of the meandering step instability. Meandering instability however differently than bunches happens in two dimensions and diffusion along step edges rather than surface diffusion can be here the main source of the kinetic asymmetry [23–26]. It acts via Schwoebel barrier at kinks or via unhindered step-edge diffusion. In our simulations of 4H-SiC(0001) we observe meandering step structure even for low rates of crystal growth, so it seems that step edge diffusion is responsible for creation of such structures. Moreover, we see that steps stay straight for higher temperatures at the same growth rates what suggests the presence of kink Schwoebel barrier. The presence of kink Schwoebel barrier can be attributed to the bonds that have to be broken when particle overcomes step kink. For higher temperatures barrier of given height results in lower differences of particle fluxes.

The particle flux balance changes when some additional factors leading to the kinetic asymmetry are present in the system. The most often studied source of imbalanced fluxes at the step is the SB - difference in barriers for the jump to the step from the upper and lower terrace. It means some additional barrier for diffusion at the upper step side [18, 37, 38]. For growing crystal such barrier causes step meandering, so it enhances all effects observed for systems without any step barriers. In order to invert this tendency and induce step bunches instead of step meanders in the growing system ISB is needed [15, 38]. Such barrier increases particle flux from the upper step side on comparing with the flux from the lower terrace. The anisotropy like that can be modeled

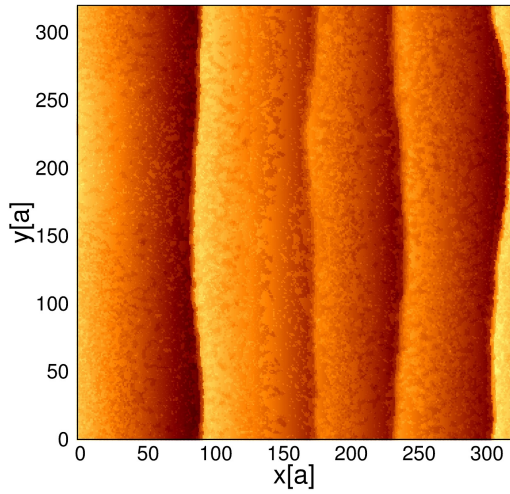


FIG. 2: Bunches at SiC surface for  $\ln(F/D) = -10$  and  $\beta = 6eV^{-1}$

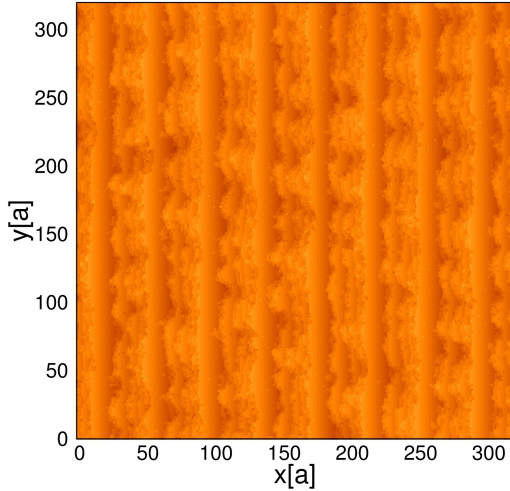


FIG. 3: 4-step structure at SiC surface for  $\ln(F/D) = -12$  and  $\beta = 4eV^{-1}$

in Monte Carlo simulation procedure either by decrease of the barrier for the diffusion of particles from the upper terrace or by increase of the barrier at the lower terrace. The second method is more effective one as it was discussed in Ref. 38. We have checked this for our systems in practice on comparing data for both realizations of particle dynamics process. The result of our simulations was that only the second method leads to the bunched patterns, whereas the first one is not. Hence in our model we use formula (4) for the particles that attach step from the lower terrace and in such a way we induce flux, which moves in opposite direction to the step-flow advection of particles during crystal growth process.

Particle fluxes along step edges and along surface can be larger or smaller depending on the step velocity, which is related to the external particle flux  $F$  and to the sur-

face miscut. On the other hand intensity of the opposite particle flux due to the ISB asymmetry depends on the temperature. For higher temperatures, factor  $\beta$  is lower and the ratio of jumps at both sides of the step decreases. Due to competition of both asymmetry factors we can expect different surface behavior for different temperature and particle fluxes. As it was discussed in Refs 1, 2 the presence of impurities of given type can induce or remove additional diffusion barrier, hence we expect that various values of effective jump barriers at the step can be realized at different growth conditions. We have checked the behavior of the model for two different diffusion barriers  $B_I$  and indeed several regions of different step patterns can be found in the  $F/\nu$  and  $\beta$  plane.

### B. Step patterns in the system with high ISB

Let us first discuss the case where high ISB was assumed for both Si and C adatoms  $B_I = 0.75eV$ . Large ISB values have been found in experimental systems, for example 1eV at Si surface [39]. Resulting diagram of different surface structures at 4H Si(100) is presented in Fig 1. On changing flux and temperature three different step arrangements can be observed. At low temperatures (high  $\beta$  values) ISB is the dominating factor and leads to the step bunching process. Steps group in bunches which join together for longer times of crystal growth [17, 40–42]. The example of such step pattern is shown in Fig. 2. Bunches are rather straight. It can be seen that they can bend slightly during their evolution. At low temperatures bunch structure was observed for all studied particle fluxes, whereas for higher temperatures two different types of straight step structures were found. When crystal is grown slowly it leads to a regular four step structure, what means that we have here stationary pattern of one unit cell multi-steps. Example of such structure is shown in Fig. 3. Difference between regular and shallow four-step structure and large bunches is clearly visible when we compare Fig 2 and Fig 3. For higher rates of crystal growth at higher temperatures we enter region of regular steps at the surface. This pattern changes its character into the rough surface when growth becomes faster. Within all parameters range no meandering was seen except small ripples at three out of four steps in 4-step structure in Fig 3. This means that high ISB, which leads to the emergence of straight bunches damps step meanderings at the same time. One of reasons that meandering instability is suppressed is the presence of ISB at kink, the same as ISB at steps. The presence of this barrier can stop the fluxes that flow along step. Similarly we do not see any domains build at terraces. This is again caused by ISB effect.

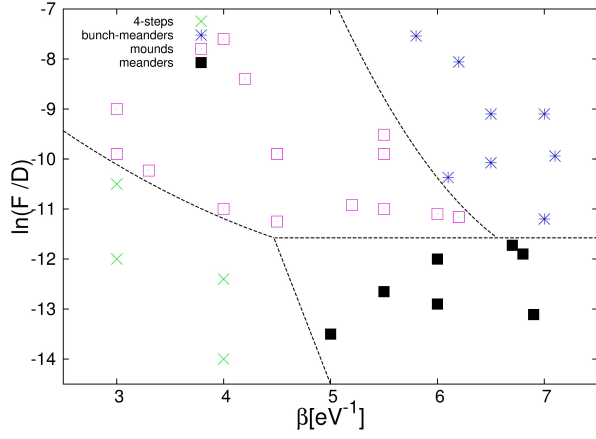


FIG. 4: Diagram of different step patterns found at SiC(0001) surface in the  $F/D$  and  $\beta$  plane calculated for the case when  $E_B^{Si} = 0.5eV$  and  $E_B^C = 0.2eV$

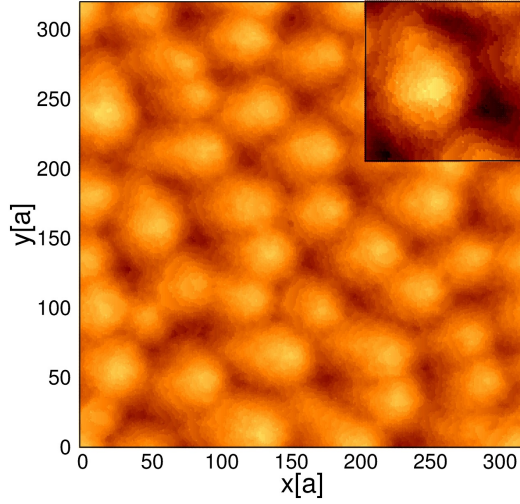


FIG. 5: Structure of mounds at SiC surface for  $\ln(F/D) = -9.9$  and  $\beta = 4.5$ . Insert shows one of mounds in close-up.

### C. Step patterns in the system with low ISB

The same range of growth parameters was studied for the system of lower values of ISB. In this case we also assumed that two barriers are different and so we have  $B_I = 0.5eV$  for C atoms and  $0.2eV$  for Si atoms. In Fig. 4 we show diagram of patterns obtained for this system. The character of this diagram does not change as long as both barriers are lower than  $0.7eV$  and stay around value  $0.4eV$ . Within the studied range of parameters four different step structures can be found. For fast crystal growth at higher temperatures mound formations can be seen. In Fig 5 characteristic round mound structures are clearly visible. When temperature decreases the structure of mounds rapidly changes and we can see elongated structures of meandered bunches (Fig 6). The difference between mound and this last ordering is appar-

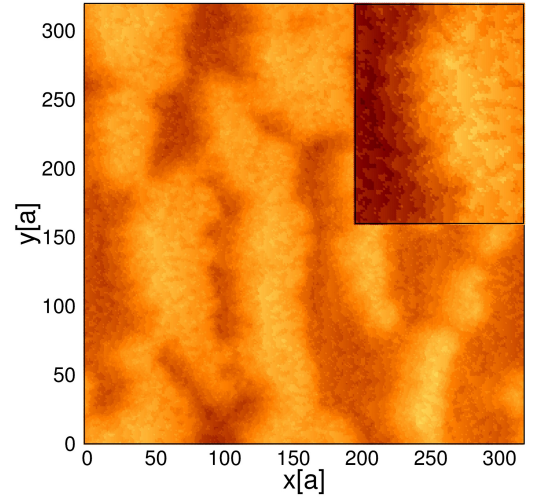


FIG. 6: Meandered and bunched structure at SiC surface for  $\ln(F/D) = -9$  and  $\beta = 6.5$ . Insert shows part of the picture in close-up.

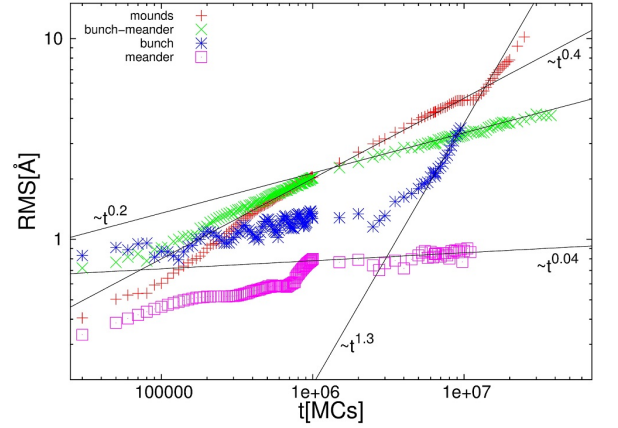


FIG. 7: Surface roughness as a function of time for different patterns, measured as root mean square of height of the surface. Successive curves describe surface patterns presented in Figs 5,6,2 and 11.

ent. The first are round regular structures, the second are elongated structures, bunched along steps. Mounds increase, glue together and as an effect roughness of the surface increases faster than this of bunch and meandered structure. The difference between roughness as a function of time for bunch and meandered structure and for mounds can be seen in Fig. 7. Presented value was calculated as a root mean square of height  $h_i$  correlation function  $RMS = \sqrt{\langle (h_i - h_0)^2 \rangle}$ , where  $h_0$  is mean surface height. It can be seen that roughness of mounds increases faster. Also the growth is not steady, roughness jumps up when some reorganization covering a large area happens at the surface. Correlation functions for both structures can be also compared in Figs. 8 and 9. Correlation function is calculated as the height correlation



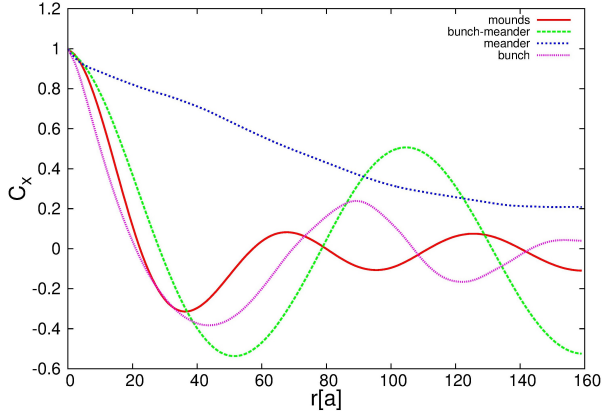


FIG. 8: Correlation function along  $x$  direction for the same surfaces as in Fig. 7 plotted at  $t = 10^7$ .

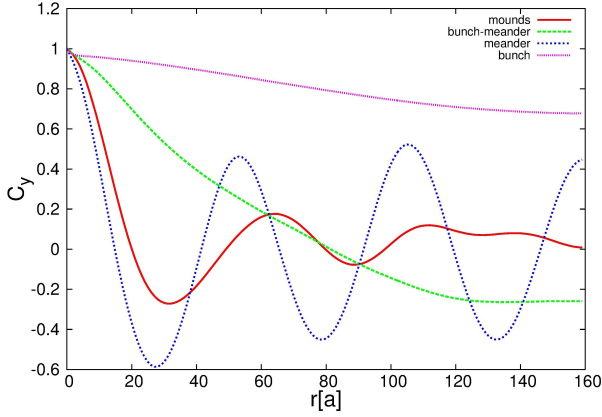


FIG. 9: Correlation function along  $y$  direction for the same surfaces as in Fig. 7 plotted at  $t = 10^7$ .

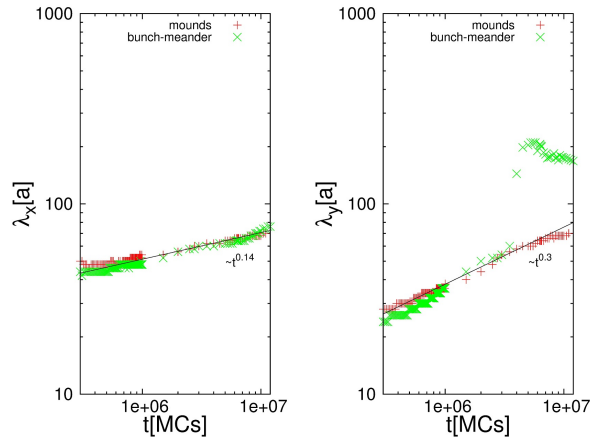


FIG. 10: Characteristic wavelength along axis  $x$  and  $y$  for mounded (Fig 5) and meandered and bunched (Fig 6) structures.

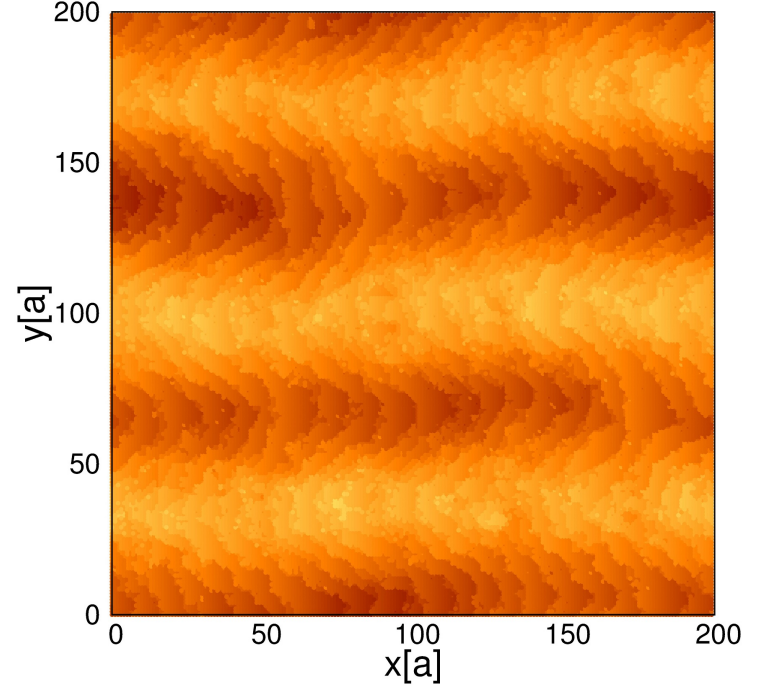


FIG. 11: Meandered structure at SiC surface for  $\ln(F/D) = -12.6$  and  $\beta = 6$ .

along  $x$  axis  $C_x = \sum_i (h_i - h_0)(h_{i-x} - h_0)$  and along  $y$  axis  $C_y = \sum_i (h_i - h_0)(h_{i-y} - h_0)$ . Correlation function for bunch and meander structure oscillates in the direction  $x$  - in the direction of step movement and shows no special structure along step direction. Oscillations in  $x$  direction are similar to these seen for correlation function of surface with bunches. When the same correlation functions are calculated for mounds oscillations of the same length are present in both directions. They are damped due to the mound size and different location. Time dependence of the correlation length measured as the position of first minimum of correlation function is shown in Fig 10. It can be seen that up to the  $4 \cdot 10^6 MC$  time steps points for mounds and bunch and meandered structures are at one curve. It means that step deformation along steps and across steps happens in the same way. Afterwards the wavelength along steps ( $y$  axis) for this second structure jumps up thus showing emergence of elongated structures in this directions - bunches.

Coexistence of bunching and meandering instability was shown in Ref.31 at metallic vicinal surfaces and several possible mechanisms were discussed there. Among these mechanisms ISB was excluded with argumentation that it leads to straight, not meandered steps due to its stabilizing effect against meandering. This effect however is not so strong when step movement together with the diffusion along steps are not neglected in the stability analysis. In Ref. 32, 33 simultaneous bunching and meandering was studying by use of phase-field model and deposition rate was a controlling parameter. This phe-

nomenon was shown to emerge as collective SB and stress due to elastic interaction. We assumed in our simulations ISB and diffusion along surface and along steps and interplay of these factors resulted in several different step patterns.

When we decrease particle flux keeping low temperatures meandered in phase structure emerges [17, 19, 43–45]. We can see this structure in Fig 11. Regular meandered patterns are realized for relatively high ISB. The particle fluxes up the steps along step edges win over ISB surface effect in this region of parameters. Roughness for this meandered pattern is much lower than the one seen in the previous examples but correlation function in Fig. 9 shows very large variability in the direction perpendicular to the step move direction. In the direction of crystal miscut the same structure is very smooth (Fig 8). Higher temperatures together with lower growth rates make step to straighten and eventually left down side part of the phase diagram is similar to this in the diagram in Fig 1 occupied by four step structure, which again builds up for low  $F$  value and high temperatures.

Two different factors play role here: the temperature and the growth rate. The system is two dimensional, so 1D models of step evolution are not complete in this case. On lowering temperature the importance of ISB barrier grows, what first of all prevents domain creation at steps. Such effect can be responsible for the transition from mounds to the meandered bunches for lower temperatures. It has to be taken also into account that on changing temperature step permeability also changes what can have dramatic results [41, 42]. Moreover the balance between kink and step edge energies changes what leads to the change of the flux balance. An interplay of all of these factors results in different step patterns for different model parameters.

#### IV. CONCLUSIONS

Kinetic Monte Carlo simulations were done for Si(0001) surface with  $8^\circ$  miscut along  $[01\bar{1}0]$  direction. Interplay between the particle flux imbalanced due to the step edge diffusion, natural step movement and this caused by the presence of ISB was studied. These factors induce net particle fluxes moving in different di-

rections. The value of flux difference induced by these factors changes with the step velocity and temperature. Step velocity depends on the crystal growth rate and the miscut angle. The importance of ISB changes with the temperature of the system. The lower temperature is, the ratio between different jumps over the surface is higher. On the other hand for the higher fluxes of particles adsorbed at the surface relations between fluxes of all types can change.

As a result on changing growth condition different surface patterns are observed, similarly as in experimental situations. Temperature and growth rate are the usual parameters changed in experiments. Morphological instability can be also induced by impurities i.e. by nitrogen [1, 2]. We show that if impurity influence onto the growth process can be treated as the change in ISB height at steps it indeed explains emergence of surface structures. Step bunching appears at rather low temperatures for relatively high ISB. This bunch structure is rather stiff and stable. When temperature increases we get the regular single step or four multi-step structure. For lower ISB bunched and meandered structure appears at low temperatures and at relatively high growth rate. This pattern changes into the in phase meandered step arrangement at lower external particle flux and into the regular mound structure at higher temperatures. At low growth rates and high temperatures steps at the surface evolve towards straight four- step structure. Transition between different structures is sharp and the character of step pattern is easy to determine. In general for higher temperatures and lower growth rates steps become more straight.

Similar phase diagrams are expected for other surface miscuts. However because step velocity increases with lower miscut, transition lines in these diagrams should be located at different flux values.

#### V. ACKNOWLEDGEMENT

This work was partially supported by research grants from the National Science Centre(NCN) of Poland (Grant NCN No. 2011/01/B/ST3/00526) and from the European Regional Development Fund, through grant Innovative Economy (POIG.01.01.02-00-008/08)

- 
- [1] N. Ohtani, M. Katsuno, J. Takahashi, H. Yashiro, and M. Kanaya Surf. Sci. 398 (1998) L3033
  - [2] N. Ohtani, M. Katsuno, J. Takahashi, H. Yashiro, and M. Kanaya, Phys. Rev. B 59 4592 (1999)
  - [3] S. Nakamura, T. Kimoto, S. Tanaka, N. Taraguchi, A. Suzuki and H. Matsunami Appl. Phys. Lett. 76, 3412 (2000)
  - [4] K. Wada, T. Kimoto, K. Nishikawa, H. Matsunami, J. Cryst. Growth 291 (2006) 370-374.
  - [5] Hiroyuki Matsunami and Tsunenobu Kimoto, Materials Science and Engineering, **R20** (1997) 125-166
  - [6] S.Omar,M.V.S. Chandrashekhar,I.A.Chowdhury,T. A. Rana, andT. S. Sudarshan J. Appl. Phys. **113**, 184904 (2013)
  - [7] M. Suvajarvi, R. Yakimova, E. Janzén, J. Cryst. Growth **236** 297 (2002);
  - [8] Yuji Yamamoto, Shunta Harada, Kazuaki Seki, Atsushi Horio, Takato Mitsuhashi, and Toru Ujihara Applied Physics Express 5 (2012) 115501
  - [9] Tsunenobu Kimoto, Akira Itoh, and Hiroyuki Mat-

- sunami Tetsuyuki Okano J. Appl. Phys., Vol. 81, No. 8, 15 April 1997
- [10] M. Yazdanfar, I. G. Ivanov, H. Pedersen, O. Kordina, and E. Janzan, Journal of Applied Physics 113, 223502 (2013);
  - [11] L. Dong, Guosheng Sun, Jun Yu, Liu Zheng, Xingfang Liu, Feng Zhang, Guoguo Yan, Xiguang Li, and Zhanguo Wang Applied Surface Science 270 (2013) 301
  - [12] T. Kato, A. Kinoshita, K. Wada, T. Nishi, E. Hozomi, H. Taniguchi, K. Fukuda, H. Okumura, Materials Science Forum 645-648 (2010) 763-765.
  - [13] B. Chen, H. Matsuhata, T. Sekiguchi, K. Ichinoseki, H. Okumura, Acta Materialia 60 (2012) 5158.
  - [14] B.L. Van Mil, K.K. Lew, R.L. Myers-Ward, R.T. Holm, D.K. Gaskill, C.R. Eddy Jr., L. Wang, P. Zhao, Journal of Crystal Growth 311 (2009) 238-243.
  - [15] Masahide Sato, Makio Uwaha, and Yukio Saito Phys.Rev.Lett. **80** (1998)
  - [16] K. Yagi, H. Minoda, and M. Degawa, Surf. Sci. Rep. **43**, 45 (2001).
  - [17] C. Misbah, O. Pierre-Louis, and Y. Saito, Rev. Mod. Phys. **82**, 981 (2010).
  - [18] R. L. Schwoebel, E.J Shipsley, J. Appl. Phys. **37** (1966) 3682
  - [19] G.S. Bales and A. Zangwill, Phys. Rev. B **41**, 5500 (1990).
  - [20] M. Dufay, T. Frisch, and J-M Debierre Phys. Rev. B, **75**, 241304(R)(2007)
  - [21] B. Ranquelov, S. Stoyanov, Phys. Rev. B **76**, 035443 (2007)
  - [22] M. A. Zauska-Kotur and F. Krzyewski, J. Appl. Phys. **111**, 114311 (2012).
  - [23] M. V. R. Murty and B. H. Cooper Phys. Rev. Lett. **83** (1999) 352.
  - [24] O. Pierre-Louis, M. R. D'Orsogna, and T.L. Einstein Phys. Rev. Lett. **82**, (1999) 3661.
  - [25] P. Politi and J. Krug, Surf. Sci. **446**, (2000) 89.
  - [26] F. Nita and A. Pimpinelli, Phys. Rev. Lett **95**, 106104 (2005).
  - [27] V. Borovikov, A. Zangwill, Phys. Rev. B 79, 245413 (2009)
  - [28] M. Camarda, Surf. Sci. 606 (2012) 1263-1267
  - [29] Massimo Camarda, Antonino La Magna, Francesco La Via, J. Comp. Physics 227 (2007) 1075-1093
  - [30] M. Camarda, A. Severino, A. LaMagna, and F. La Via AIP Conf. Proc. 1292, 19 (2010)
  - [31] N. Neel, T. Maroutian, L. Douillard, and H-J Ernst Phys. Rev. Lett. **91** 226103 (2003)
  - [32] Y. M. Yu, A Voigt, X Guo, and Y. Liu, Appl. Phys. Lett. **99**, 263106 (2011)
  - [33] Y-M Yu, B-G Liu Phys Rev B **73**, 035416 (2006).
  - [34] G. Cicero and A. Catellani, Appl. Surf. Sci **184** 113 (2001)
  - [35] Q. A. Bhatti and C. C. Matthai, Thin Solid Films, **318** 46 (1998)
  - [36] Borysiuk et. al. Phys. Rev. B **85** 045426 (2012)
  - [37] M Sato, M Uwaha, Surf. Sci. 493 (2001) 494-498
  - [38] M.H. Xie, S.Y. Leung, S.Y. Tong Surface Science 515 (2002) L459-L463
  - [39] D. I. Rogilo, L. I. Fedina, S. S. Kosolobov, B. S. Ranguelov, and A.V. Latyshev, Phys. Rev. Lett. **111**, 036105 (2013)
  - [40] H. Omi, Y. Homma, V. Tonchev, A. Pimpinelli Phys. Rev. Lett. **95** 216101 (2005).
  - [41] S. Stoyanov and V Tonchev, Phys. Rev. B **58**, 1590 (1998)
  - [42] M. Sato, M. Uwaha, and Y. Saito, Phys. Rev. B **62**, 8452 (2000).
  - [43] O. Pierre-Louis, C. Misbah, Y Saito, J. Krug, and P. Politi, Phys. Rev. Lett. **80** 4221 (1998).
  - [44] I. Bena, C. Misbah, and A. Valence, Phys. Rev. B **47**, 7408 (1993).
  - [45] M.A. Zaluska-Kotur, F. Krzyzewski, S. Krukowski, J. Appl. Phys. **109**, 023515 (2011).